COAXIAL COUPLER RF KICK IN THE PITZ RF GUN.

Y. Chen†, H. Qian, M. Krasilnikov, I. Isaev, Q. Zhao[1], P. Boonpornprasert, J. Good, H. Huck, Y. Renier, A. Oppelt, and F. Stephan,
DESY, Platanenallee 6, 15738 Zeuthen, Germany
W. Ackermann, TEMF, Technische Universität Darmstadt, Schlossgartenstraße 8, 64289 Darmstadt, Germany
M. Dohlus, DESY, Notkestraße 85, 22607 Hamburg, Germany
† ye.lining.chen@desy.de   [1] on leave from IMP/CAS, Lanzhou, China

INTRODUCTION

We investigate a transverse RF kick induced by the transition between rectangular waveguide and coaxial line of the RF coupler in the 1.6-cell L-band normal conducting (NC) RF gun at the Photo Injector Test Facility at DESY, Zeuthen site (PITZ). A three-dimensional electromagnetic simulation shows the disturbed RF field distributions in the fundamental accelerating mode. Based on the 3D RF field map, an electron beam based characterization and quantification of the coaxial coupler RF kick in the PITZ gun is simulated. Preliminary results of the investigations are presented.

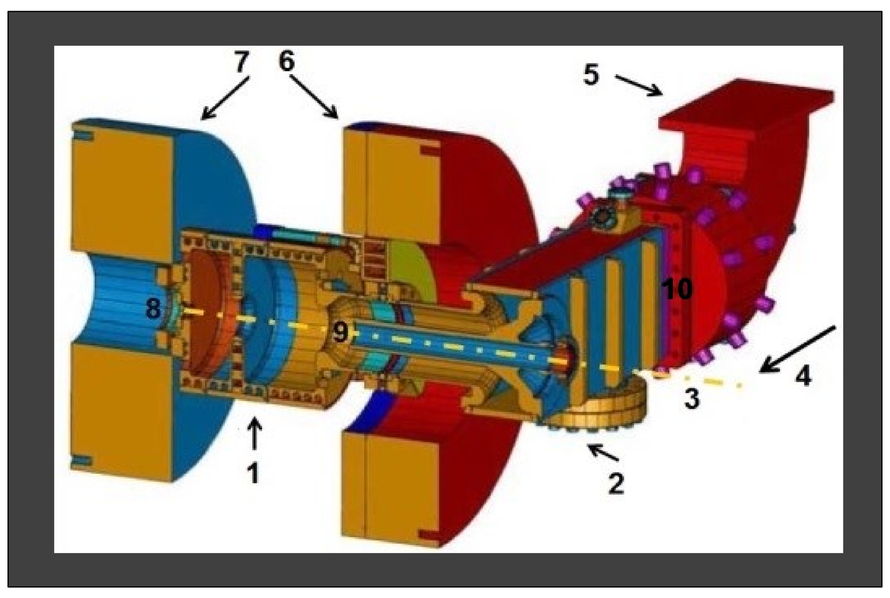

Figure 1: Sketch of the PITZ gun with coaxial RF coupler: 1-gun cavity, 2-door-knob transition, 3-cavity axis, 4-RF feeding direction, 5-input WG, 6-main solenoid, 7-bucking solenoid, 8-cathode, 9-end of coaxial line and 10-reference position of WG port for simulations. Note that, compared to the computational model used in simulations, this sketch is rotated by 90 degrees.

RF FIELD ASYMMETRY

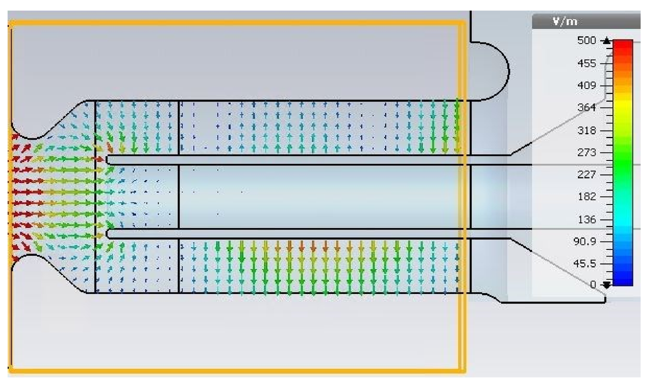

(a) Cut-plane view of E-vector

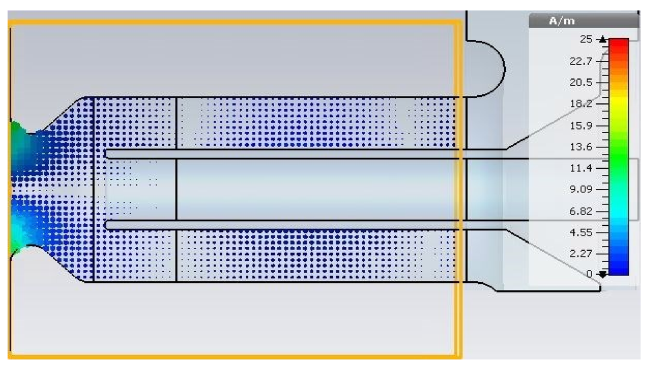

(b) Cut-plane view of H-vector

Figure 2: Illustration of the local RF field asymmetries. The colour maps are adjusted for a better visualization.

The RF field in the gun is simulated using the frequency domain solver in the CST-MWS®. To enable excitation, a standard WG port condition is applied at the boundary of the input WG. Based on a so-called mono-frequency excitation method, two principal matching conditions (i.e., broadband matching from WG to coaxial line and narrowband matching from coaxial line to cavity) are satisfied by slightly tuning the length of the inner conductor. This results in a reflection coefficient lower than -30 dB at the WG port position. The RF field is then calculated under such optimized conditions of the gun at its resonance frequency. Surface losses are taken into account.

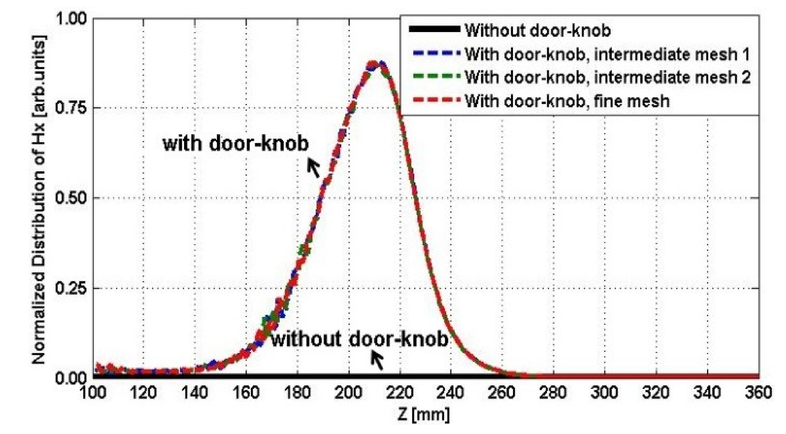

Figure 3: Distribution of the magnetic field component (Hx) along the cavity axis of symmetry and the comparison with the same field calculated by the simulation without door-knob transition in the computational model. Different curves in blue, green and red represent gradual steps for mesh refinements in the simulations.

BEAM-BASED CHARACTERIZATION OF THE RF KICK

The kick characterization is conducted by scanning the RF start-phase of the gun in particle tracking simulations. The beam centroid on track is initially placed at the center of the cathode plane. It is tracked through the gun cavity till close vicinity of the door-knob transition. The whole calculation domain is covered by the RF field map.

In Fig. 4, the particle off-center distance (i.e., in (a) and (b)) on the transverse plane and corresponding transverse momentum (i.e., in (c) and (d)) are calculated at different longitudinal positions along the cavity axis of symmetry. In Fig. 5, the kick strength and the off-center displacement at z = 0.3 m are plotted as a function of the gun phase.

Note that, a nominal electron bunch of 20 ps in FWHM (full width half maximum) at PITZ corresponds to about 10 degrees gun phase at the resonant frequency of 1.3 GHz. Consequently, the head and tail of the electron bunch may see a kick slope (see (b) in Fig. 5) due to the time dependency of the RF kick. This results in a kick difference of 0.05 mrad around the MMMG phase. However, the presence of the solenoid field may further complicate the dynamics [15-17].

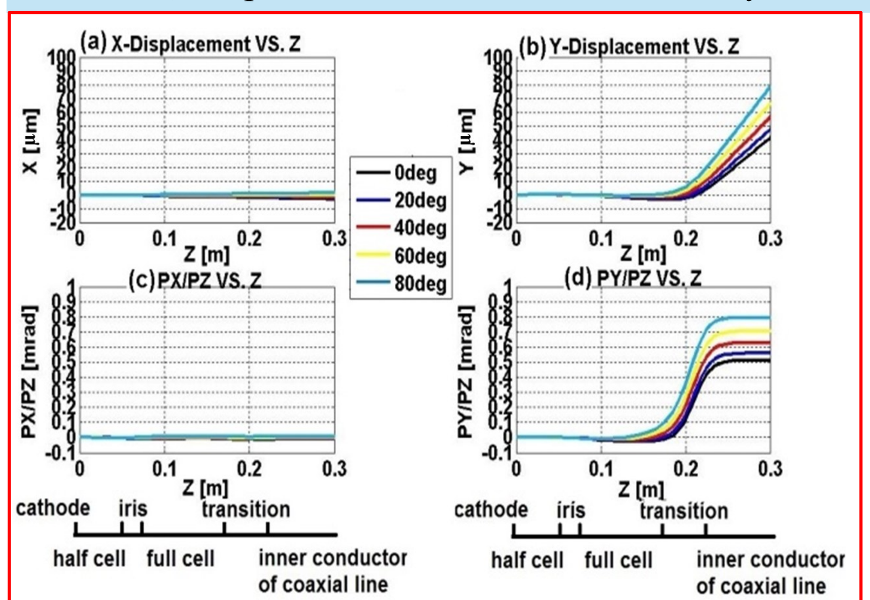

Figure 4: Off-center distance on the transverse plane and corresponding transverse momentum of the beam centroid on track for the RF phases between -40 and 40 degrees w.r.t. MMMG phase of the gun.

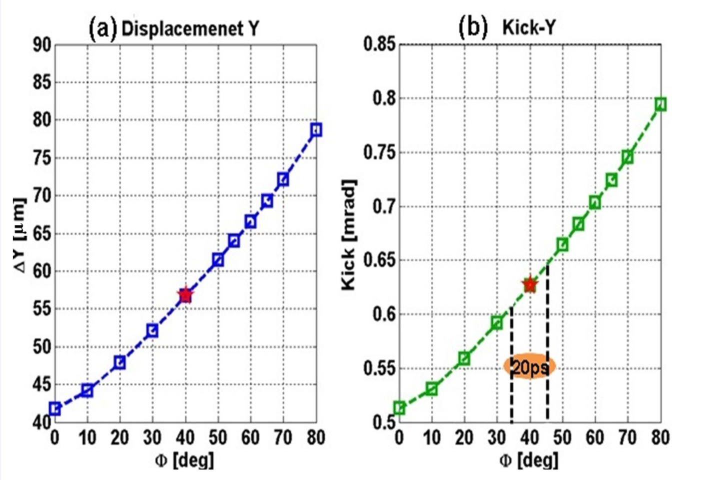

Figure 5: Vertical displacement at z = 0.3 m and kick strength as a function of the gun phase.

MULTIPOLE EXPANSION BASED KICK QUANTIFICATION

To clarify the multipole composition and quantify their strengths in the integral kick, the transverse momentum of the beam particle is presumably decomposed as a dipole component, a normal and a skew quadrupole component in (1) and (2).

$$P_X = P_{0x} + (K_{RF} + K_N)X + K_S Y \quad (1) \qquad P_Y = P_{0y} + (K_{RF} - K_N)Y + K_S X \quad (2)$$

X and Y are the off-center distance at the location of the integral kick, respectively. P_X and P_Y represent particle transverse momentum in the horizontal and vertical direction, respectively. P_{0x} (or P_{0y}) characterizes the dipole kick. K_{RF} is the RF focusing strength of the cylindrical symmetric mode. K_N and K_s denotes the normal and skew quadrupole kick strength, respectively.

The particle tracking simulation results used to fit the formulas (1-2) are shown in Fig.7. The initial positions on the cathode plane of all on-track particles in the simulations are illustrated in Fig. 6.

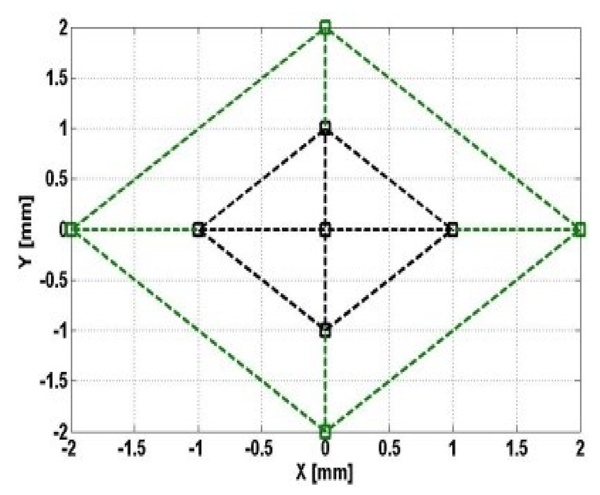

Figure 6: Beam centroid positions on the cathode plane used in the simulations for kick quantification.

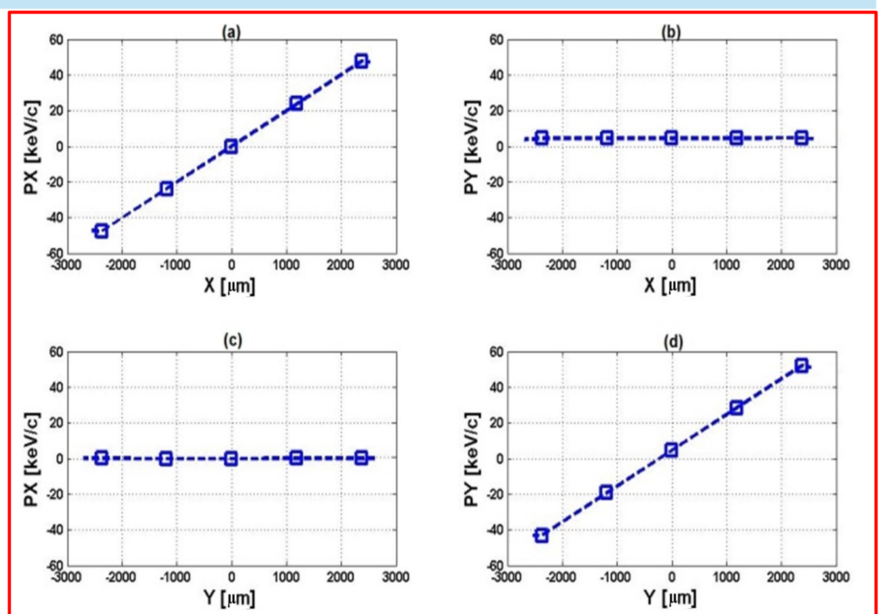

Figure 7: Particle tracking simulation results for multipole expansion based quantification of the integral kick.

Based on the simulation results in Fig. 7, the multipole expansion forms (1-2) are numerically fitted. **This renders a horizontal dipole kick (P_{0x}) of 0.007 keV/c and a vertical dipole kick (P_{0y}) of 4.576 keV/c. For the normal quadrupole component, the kick strength K_N is estimated as 1.0e-5 keV/c/µm. The skew quadrupole component, meanwhile, is calibrated by K_S as 5.0e-6 keV/c/µm.**

To cross-check the kick quantification, **an electron bunch of 20 ps in FWHM with temporally flattop shape is used for tracking simulations, instead of beam centroids.** Fig. 8 shows the vertical kick strength (PY/PZ) as a function of the longitudinal positions for the electron bunch distribution at z ≈ 0.33 m (blue dots). To visualize the kick variation in time, the whole bunch is treated slice by slice (dashed black lines). Within each slice, the mean kick strength is calculated. Fig.8 (b) provides a closer look at the trend of the kick slope along the bunch. One can see, that the mean kick strength is about 0.65 mrad, and also, that the bunch tail sees higher kick strength than the head by approximately 0.05 mrad. This is **consistent as in Figs. 4 and 5.** Note once again that, the beam dynamics may be further complicated due to the presence of the space charge force and the solenoid field [15-17].

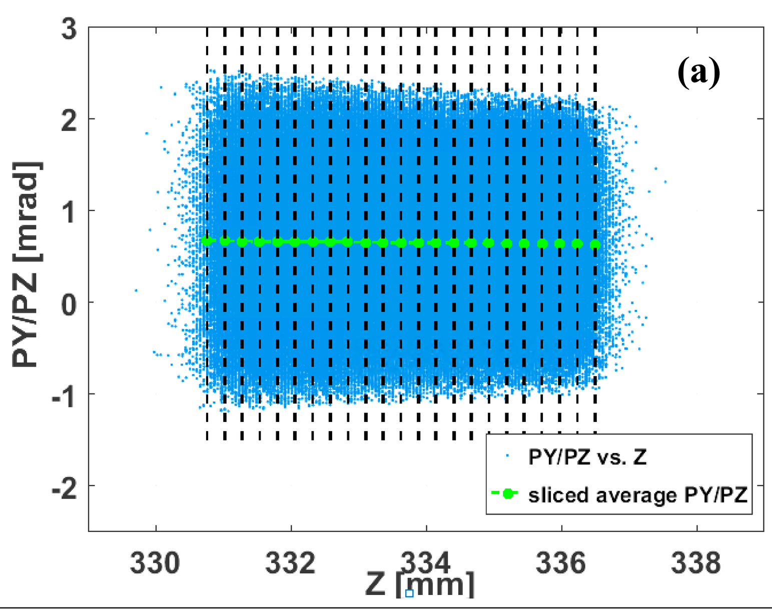

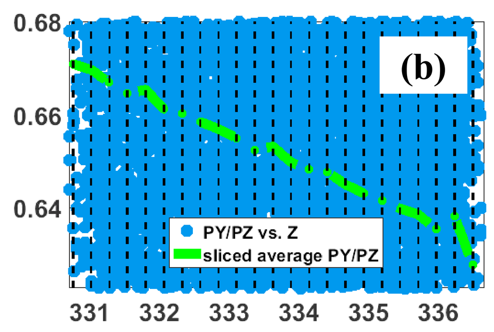

Figure 8: Bunch distribution at z ≈ 0.33 m in terms of the vertical kick strength (PY/PZ) versus z-positions and slice parameters of the kick. **(b) is a zoomed-in image of the central part of the main figure (a).**

SUMMARY AND OUTLOOK

In this paper the RF fields with rotational symmetry disturbed by the transition from the input rectangular waveguide to the coaxial coupler of the PITZ gun are shown. **The resulting RF kick to the electron bunch is vertical and time-dependent.** The latter characteristic can introduce a kick slope along the bunch. The integral kick is, furthermore, quantified in the form of its multipole components using the results of particle tracking simulations. **This gives a main dipole kick of about 0.65 mrad at the MMMG phase of the gun for a gun RF power of 6.5 MW.** A small normal and skew quadrupole component is found to be about 1.0e-5 keV/c/µm and 5.0e-6 keV/c/µm, respectively.

Further studies are foreseen to investigate the impacts of the kick on the beam dynamics when the space charge effect is included. **Note also that, to explain the asymmetries in measured transverse phase spaces and transverse profiles of the electron bunch at PITZ, other effects, such as the imperfect solenoid symmetry are also under investigation (cf. [15-17]).**

REFERENCES

1. W. Ackermann et al., Operation of a free-electron laser from the extreme ultraviolet to the water window. Nat. Photon. 1, 336, 2007.
2. M. Altarelli et al., DESY, Hamburg, Report No. DESY 2006-097, 2006.
3. F. Stephan, C. H. Boulware, M. Krasilnikov et al., Detailed characterization of electron sources yielding first demonstration of European X-ray Free-Electron Laser beam quality. PRSTAB 13, 020704, 2010.
4. M. Krasilnikov, F. Stephan, G. Asova et al., Experimentally minimized beam emittance from an L-band photoinjector. PRSTAB 15, 100701, 2012.
5. Y. Renier et al., "Statistics on high average power operation and results from the electron beam characterization at PITZ", IPAC'17, Copenhagen, Denmark, TUPIK051, p.1806 (2017).
6. F. Stephan and M. Krasilnikov, Synchrotron Light Sources and Free-Electron Lasers, Charpter: High Brightness Photo Injectors for Brilliant Light Sources (Springer International Publishing Switzerland, 2016), ISBN 9783319143941.
7. B. Dwersteg, K. Flottmann, J. Sekutowicz et al., RF gun design for the TESLA VUV Free Electron Laser, NIM A393, 93-95, 1997.
8. F. B. Kiewiet et al., "A DC/RF gun for generating ultra-short high brightness electron bunches", EPAC'00, Vienna, Austria, p.1660 (2000).
9. A. Oppelt et al., "Tuning, conditioning, and dark current measurements of a new gun cavity at PITZ", FEL'06, BESSY, Berlin, Germany, THPPH023, p. 609 (2006).
10. M. Krasilnikov et al., "Impact of the RF-Gun Power Coupler on Beam Dynamics", EPAC'02, Paris, France, p. 1640 (2002).
11. M. Dohlus et al., "Coupler kick for very short bunches and its compensation", EPAC'08, Genoa, Italy, p. 580 (2008).
12. H. Qian et al., "Design of a 1.3 GHz Buncher for APEX", IPAC'14, Dresden, Germany, THPRI066, p. 3924 (2014).
13. CST Computer Simulation Technology AG, https://www.cst.com/.
14. K. Floettmann, ASTRA particle tracking code, http://www.desy.de/~mpyflo/.
15. M. Krasilnikov et al., "Investigations on Electron Beam Imperfections at PITZ," LINAC'16, East Lansing, MI, USA, MOPLR013, p. 165 (2016).
16. M. Krasilnikov et al., "Electron beam asymmetry compensation with gun quadrupoles at PITZ", these proceedings.
17. Q. Zhao et al., "Beam asymmetry studies with quadrupole field errors in the PITZ gun section", these proceedings.

European XFEL

FLASH. Free Electron Laser in Hamburg

PITZ Photo Injector Test Facility at DESY, Location Zeuthen (PITZ)